Available online at www.sciencedirect.com
SCIENCE DIRECT®
Journal of Sound and Vibration 280 (2005) 41–61
JOURNAL OF SOUND AND VIBRATION
www.elsevier.com/locate/jsvi

Experimental force estimation in a constrained vibrating structure using modal-based methods

N. Sehlstedt*, M. Dalenbring

Department of Computational Physics, Aeronautics Division, FFA Swedish Defence Research Agency, SE-172 90 Stockholm, Sweden

Received 20 January 2003; accepted 24 November 2003

Abstract

In this paper three recently developed traction vector techniques will be experimentally validated. Common ground for the techniques are based on a modal expansion of the displacement field and utilization of sets of normal eigenmodes and displacement measurements in order to yield detailed descriptions of the traction vector field acting at the boundary. Comparison between the methods is made regarding the experimental estimation of traction vectors both point-wise and in an L_2-norm over the boundary in question. The results are good especially regarding the normed results.
© 2004 Elsevier Ltd. All rights reserved.

1. Introduction

The estimation of boundary traction vector (or excitation/reaction force) acting on a vibrating structure is an important research field within the discipline of structural dynamics. Recently three separate methods for solving the problem of boundary traction vector estimation from observed vibration response where proposed, see Refs. [1–3]. This problem is, in the literature, usually referred to as the inverse problem, see e.g., the review article by Dobson and Rider [4]. Solving the inverse problem is theoretically straightforward. However, it often turns out that the system of equations which arise, is numerically ill-conditioned, i.e., the equation matrix has a high condition number. This can yield highly inaccurate results due to noise in the measured data. Therefore well-conditioned approaches for solving the inverse problem are highly desirable. One possible way to improve the condition number may be to use Tikhonov regularization (or damped least squares). Examples of applications using regularization can be seen in e.g., Refs. [5–7]. This approach adds a penalty to a least square formulation of the problem. However, while regularization improves

*Corresponding author. Fax: +46-8-55504306.
E-mail address: stn@foi.se (N. Sehlstedt).

0022-460X/$ - see front matter © 2004 Elsevier Ltd. All rights reserved.
doi:10.1016/j.jsv.2003.11.065

the condition number it has the drawback in that it needs to smooth the solution in such way that cannot be predicted beforehand.

Bartlett and Flannelly [8] use a technique called force determination method for determination of vibratory hub forces on a helicopter. Starkey and Merrill [9] proposed two algorithms for the solution of the inverse problem. The first one involves the use of a frequency-dependent pseudo-inverse of the acceleration matrix, hence the inverse must be calculated for each frequency of interest. The acceleration matrix is defined as the matrix relating Fourier transforms of the acceleration and force vectors. The second algorithm is based on vibration eigenmodes and involves pseudo-inverses of the modal matrix and a sub-matrix of the modal matrix. Starkey and Merrill also conducted a perturbation investigation and concluded that the condition number of the acceleration matrix is a good estimate of force errors. The second algorithm was also studied by Hansen and Starkey [10]. In Ref. [11] a point force identification problem for a simply supported plate, where the location, phase and magnitude of the force is unknown, was considered. Möller [12] studied the ill-posed version of the inverse problem for a discrete system, where not even the locations of the applied loads are known. An optimization algorithm that uses the Betti reciprocal theorem, added discrete masses and additional response measurements is proposed.

In Ref. [1] it was shown that the ill-conditioned system of equations, that often arises when solving the inverse problem, using modal-based techniques, is caused by the well-known fact that modes, orthogonal in a volume, are in general not orthogonal in a subspace of the volume, such as, e.g., a boundary. One way to overcome the ill-conditioning, which was proposed in Ref. [1], is to choose a subset of the set of available modes which are orthogonal over the boundary in question. The final traction estimation step in Ref. [1] used an FE-interpolation.

In Ref. [2] the idea of well-conditioned traction estimation, as proposed in Ref. [1], was again used for the traction estimation; however, the novelty compared to Ref. [1] is that the final estimation step use a series expansion of the stress tensor. Finally in Ref. [3] the idea of Refs. [1,2] was again utilized, but here the final estimation step use a surface orthogonal basis, obtained by construction.

In this paper the three aforementioned traction techniques will be validated on an experimental test case. The details of the techniques is briefly outlined in Sections 2 and 3. In Section 4, the results of the experimental test case is presented.

Throughout the text the three-dimensional displacement field in the time domain is denoted by $\mathbf{u}(\mathbf{x}, t)$, and its frequency domain, Laplace transformed, counterpart is denoted with a *tilde* above the function, i.e., $\tilde{\mathbf{u}}(\mathbf{x}, s)$. Here, and in the following, $s = \mathrm{i}\omega$ is a complex frequency variable where i, $\mathrm{i}^2 = -1$, denotes the imaginary unit and $\omega = 2\pi \cdot f$ is the circular frequency [rad/s] of vibration; also, Hilbert space basis functions and elastic (normal) displacement (eigen-) modes are used synonymously.

2. Theory

2.1. Basic constitutive relation and equations of motion

The case of a three-dimensional, materially homogeneous solid occupying a bounded volume, $\Omega \subset \mathbb{R}^3$, will be studied. Let the boundary of Ω be denoted by $\partial\Omega$. Let also the time domain three-dimensional displacement field of the body be denoted by $\mathbf{u} = \mathbf{u}(\mathbf{x}, t)$, where $\mathbf{x} \in \Omega$ is

a point in the body, and $t \in \mathbb{R}$ is the time variable. Assuming vanishing body forces, the time domain, Cauchy's first equations of motion in the local form are given by

$$-\operatorname{div} \boldsymbol{\sigma} + \rho \ddot{\mathbf{u}} = \mathbf{0}, \tag{1}$$

where $\operatorname{div} \boldsymbol{\sigma} = (\nabla \cdot \boldsymbol{\sigma})^{\mathrm{T}}$ and ∇ is the usual gradient operator; $\boldsymbol{\sigma} = \boldsymbol{\sigma}(\mathbf{x}, t)$ is the spatial- and time-dependent second order stress tensor, and $\rho = \rho(\mathbf{x}, t)$ is the spatial- and time-dependent mass distribution in the body; in the following it is assumed that the mass distribution is time invariant, hence $\rho(\mathbf{x}, t) = \rho(\mathbf{x})$.

Assuming homogeneous initial conditions for the displacement field and the corresponding velocity field, the Laplace transformed, frequency domain counterpart to Eq. (1) can be stated as

$$-\operatorname{div} \tilde{\boldsymbol{\sigma}} + s^2 \rho \tilde{\mathbf{u}} = \mathbf{0}, \tag{2}$$

where $\tilde{\boldsymbol{\sigma}} = \tilde{\boldsymbol{\sigma}}(\mathbf{x}, s)$ and $\tilde{\mathbf{u}} = \tilde{\mathbf{u}}(\mathbf{x}, s)$ are the frequency domain stress tensor and displacement fields, respectively.

For a linear material at isothermal, but otherwise general, conditions, the frequency domain stress–strain relationship can be described by (cf., Ref. [13])

$$\tilde{\boldsymbol{\sigma}} = \mathscr{H} : \tilde{\boldsymbol{\varepsilon}}, \tag{3}$$

where $\mathscr{H} = \mathscr{H}(\mathbf{x}, s)$ is a complex, position and frequency dependent, constitutive fourth order material tensor; $\tilde{\boldsymbol{\varepsilon}} = \tilde{\boldsymbol{\varepsilon}}(\mathbf{x}, s)$ is the frequency domain (second order) strain tensor field, as defined in Appendix A; the operator :, in the above equation, denotes the double contraction between the fourth order tensor, $\mathscr{H}$, and the second order tensor, $\tilde{\boldsymbol{\varepsilon}}$, (cf., Ref. [14]). Without loss of generality, for an elastic solid, it is assumed that $\mathscr{H}$ can be decomposed as

$$\mathscr{H} = \mathscr{H}_e + \mathscr{H}_a, \tag{4}$$

where $\mathscr{H}_e$ and $\mathscr{H}_a$ denote the zero frequency, relaxed elastic properties, and the frequency-dependent viscoelastic properties, respectively. Methods for estimating the viscoelastic properties in $\mathscr{H}_a$, for a specific isotropic material, are described in Ref. [15]. The elastic compliance tensor corresponding to the elastic material tensor, $\mathscr{H}_e$, is defined as

$$\mathscr{C}_e := \mathscr{H}_e^{-1}. \tag{5}$$

The spatial- and time-dependent Cauchy (surface) traction vector is defined as

$$\mathbf{t}_n(\mathbf{x}, t) := \boldsymbol{\sigma}\mathbf{n}, \tag{6}$$

where $\mathbf{n} \in \mathbb{R}^3$ denotes the unit normal vector, to the surface. The Laplace transformed counterpart to Eq. (6) is defined as

$$\tilde{\mathbf{t}}_n(\mathbf{x}, s) := \tilde{\boldsymbol{\sigma}}\mathbf{n} = (\mathscr{H} : \tilde{\boldsymbol{\varepsilon}})\mathbf{n}. \tag{7}$$

2.2. Modal series

Let the Laplace transformed (frequency domain) displacement field, $\tilde{\mathbf{u}}$, be represented by a generalized spatial Fourier series

$$\tilde{\mathbf{u}}(\mathbf{x}, s) = \sum_{k=1}^{\infty} c_k(\tilde{\mathbf{u}}) \mathbf{w}_u^{(k)}(\mathbf{x}), \tag{8}$$

where $\mathbf{w}_u^{(k)}(\mathbf{x})$ is the elastic displacement mode number k which is the solution to the elastic eigenvalue problem Eqs. (A.12)–(A.14) given in Appendix A. The index u denotes that $\{\mathbf{w}_u^{(k)}\}_{k=1}^{\infty}$ is a basis for the displacement series in Eq. (8).

The s-dependent, i.e., frequency dependent coefficients $c_k(\tilde{\mathbf{u}})$, in Eq. (8), are linear functionals of the Laplace transformed displacement field $\tilde{\mathbf{u}}(\mathbf{x}, s)$ defined as

$$c_k(\tilde{\mathbf{u}}) \coloneqq \frac{(\tilde{\mathbf{u}}, \rho \mathbf{w}_u^{(k)})_{\mathrm{L}_2(\Omega)}}{m_k}, \tag{9}$$

$$m_k \coloneqq (\mathbf{w}_u^{(k)}, \rho \mathbf{w}_u^{(k)})_{\mathrm{L}_2(\Omega)} > 0. \tag{10}$$

Analogous to the above the frequency domain stress tensor, $\tilde{\boldsymbol{\sigma}} = \tilde{\boldsymbol{\sigma}}(\mathbf{x}, s)$ can be represented by a generalized Fourier series, cf., Ref. [16]

$$\tilde{\boldsymbol{\sigma}} = \sum_{l=1}^{\infty} g_l(\tilde{\boldsymbol{\sigma}}) \boldsymbol{\sigma}^{(l)}(\mathbf{x}), \tag{11}$$

where $\boldsymbol{\sigma}^{(l)}$ is the elastic stress tensor basis function defined as

$$\boldsymbol{\sigma}^{(l)}(\mathbf{x}) \coloneqq \mathscr{H}_e : \boldsymbol{\varepsilon}_\sigma^{(l)}, \tag{12}$$

where $\boldsymbol{\varepsilon}_\sigma^{(l)} = \boldsymbol{\varepsilon}_\sigma^{(l)}(\mathbf{w}_\sigma^{(l)})$ is the elastic strain tensor basis function, obtained here from the elastic displacement mode, $\mathbf{w}_\sigma^{(l)}$, as

$$\boldsymbol{\varepsilon}_\sigma^{(l)} = \tfrac{1}{2}[(\nabla \otimes \mathbf{w}_\sigma^{(l)})^{\mathrm{T}} + \nabla \otimes \mathbf{w}_\sigma^{(l)}]. \tag{13}$$

The index σ on $\mathbf{w}_\sigma^{(l)}$ denotes that $\{\mathbf{w}_\sigma^{(l)}\}_{l=1}^{\infty}$ is used to determine the basis $\{\boldsymbol{\sigma}_{l=1}^{\infty}\}$ for the stress series. Note that no material discontinuities may be present in Ω. Note also that Eqs. (11) and (12) together with displacement-based strains in Eq. (13) may not in some cases be a convergent (infinite) series. This is due to the fact that termwise differentiation is not always possible for infinite series in general. The demand is that the sequence must converge uniformly in order to obtain convergent derivatives.

The Fourier coefficients, $g_l(\tilde{\boldsymbol{\sigma}})$, in Eq. (11) are defined as

$$g_l(\tilde{\boldsymbol{\sigma}}) \coloneqq \frac{(\tilde{\boldsymbol{\sigma}}, \mathscr{C}_e \boldsymbol{\sigma}^{(l)})_{\mathrm{L}_2(\Omega)}}{a_l}, \tag{14}$$

$$a_l \coloneqq (\boldsymbol{\sigma}^{(l)}, \mathscr{C}_e \boldsymbol{\sigma}^{(l)})_{\mathrm{L}_2(\Omega)}. \tag{15}$$

The notation of $(\cdot,\cdot)_{\mathrm{L}_2(\Omega)}$, in the above equation, is the inner product for tensors of the same order, as defined in Appendix A. Here the order of the tensor is two.

The elastic displacement modes, $\mathbf{w}_u^{(k)}$ and $\mathbf{w}_\sigma^{(l)}$, in Eqs. (8) and (13), respectively, are two complimentary solutions to the eigenvalue problem, Eq. (A.12) with boundary conditions in Eqs. (A.13) and (A.14), on different $\partial\Omega_t$ and $\partial\Omega_w$.

It is important to note that the basis functions, for the series expansions in Eqs. (8) and (11), are considered as purely mathematical ones. This means that the boundary conditions for the eigenvalue problem have no physical meaning. Regarding the displacement series, Eq. (8), the boundary conditions for the eigenvalue problem must be such that the eigenmodes can represent some movement at the surface of interest. This means that at the surface where the traction vector is sought the boundary conditions must be pure Neumann in this case. For the stress series,

Eq. (11), the same is valid for the stress basis functions, i.e., the boundary conditions for the eigenvalue problem must be such that the stress basis functions can represent non-zero stress tensor components. This is obtained with pure Dirichlet boundary conditions (for the displacement $\mathbf{w}_\sigma^{(l)}$) at the surface of interest.

2.3. Surface orthogonal basis construction

An important fact is that a complete orthogonal set of three-dimensional basis functions in the Hilbert space $L_2(\Omega)$, i.e., the space of square integrable functions in the domain Ω, is not in general orthogonal over some part of (or the whole) the surface of the domain Ω. However, given that set of three-dimensional basis functions, a set of orthogonal (and normalized) three-dimensional basis functions can be constructed by means of Gram–Schmidt orthogonalization, an inner-product for the surface of interest and the corresponding norm.

Let $\partial\Omega_c$, $\partial\Omega_c \subseteq \partial\Omega$, denote some part of the surface, and let $(\mathbf{u},\mathbf{v})_{L_2(\partial\Omega_c)}$ and $\|\mathbf{u}\|_{L_2(\partial\Omega_c)}$ denote the $L_2(\partial\Omega_c)$-inner product and norm, respectively; both defined in Appendix A. Then, as proposed in Ref. [3], given a set of three-dimensional eigenmodes, $\{\mathbf{w}^{(k)}\}_{k=1}^{\infty}$, which are orthogonal in the volume Ω, a sequence of orthogonal and normalized basis functions, $\{\mathbf{v}^{(k)}\}_{k=1}^{\infty}$, can be obtained by the following construction:

$$\mathbf{v}^{(1)} = \frac{\mathbf{w}^{(1)}}{\|\mathbf{w}^{(1)}\|_{L_2(\partial\Omega_c)}}, \tag{16}$$

$$\left.\begin{aligned} \mathbf{f}^{(k)} &= \mathbf{w}^{(k)} - \textstyle\sum_{l=1}^{k-1} (\mathbf{w}^{(k)}, \mathbf{v}^{(l)})_{L_2(\partial\Omega_c)} \mathbf{v}^{(l)} \\ \mathbf{v}^{(k)} &= \frac{\mathbf{f}^{(k)}}{\|\mathbf{f}^{(k)}\|_{L_2(\partial\Omega_c)}} \end{aligned}\right\}, \quad k = 2, \ldots, \infty, \tag{17}$$

given the following restrictions: $\|\mathbf{w}^{(1)}\|_{L_2(\partial\Omega_c)} \neq 0$ and $\|\mathbf{f}^{(k)}\|_{L_2(\partial\Omega_c)} \neq 0$ for all $k = 2, \ldots, \infty$.

Orthogonality is here, of course, with respect to the $L_2(\partial\Omega_c)$-inner product.

2.4. Response model

By taking the L_2-inner product between Eq. (2) and $\mathbf{w}^{(k)}$, using the definition (9), Eq. (3) and Gauss' theorem it follows that

$$s^2 m_k c_k(\tilde{\mathbf{u}}) + ((\mathscr{H} : \tilde{\boldsymbol{\varepsilon}}), \nabla \otimes \mathbf{w}^{(k)})_{L_2(\Omega)} = F^{(k)}(s), \tag{18}$$

where the frequency-dependent modal force $F^{(k)}(s)$ is defined as

$$F^{(k)}(s) \coloneqq (\tilde{\mathbf{t}}_n, \mathbf{w}^{(k)})_{L_2(\partial\Omega)}. \tag{19}$$

Now, without loss of generality, assume that no material damping is present, i.e. $\mathscr{H}_a \equiv \mathbf{0}$, in Eq. (4), $\forall \mathbf{x} \in \Omega$. This will simplify the response model as will be derived below, to give a clearer view of the key issue in this paper. Then Eq. (18) is such that

$$s^2 m_k c_k(\tilde{\mathbf{u}}) + ((\mathscr{H}_e : \tilde{\boldsymbol{\varepsilon}}), \nabla \otimes \mathbf{w}^{(k)})_{L_2(\Omega)} = F^{(k)}(s). \tag{20}$$

Taking the L_2-inner product between the displacement field, $\tilde{\mathbf{u}}$, and the elastic equations of motion in Eq. (A.12) yields

$$((\mathscr{H}_e : \boldsymbol{\varepsilon}^{(k)}), \nabla \otimes \tilde{\mathbf{u}})_{L_2(\Omega)} = m_k \omega_k^2 c_k(\tilde{\mathbf{u}}), \tag{21}$$

where $\boldsymbol{\varepsilon}^{(k)}$ is the strain mode corresponding to the displacement mode $\mathbf{w}^{(k)}$ according to Eq. (A.15).

Using the properties of the inner-product of second order tensors (and major symmetry of $\mathscr{H}_e$), it can be shown that

$$((\mathscr{H}_e : \tilde{\boldsymbol{\varepsilon}}), \nabla \otimes \mathbf{w}^{(k)})_{L_2(\Omega)} = ((\mathscr{H}_e : \boldsymbol{\varepsilon}^{(k)}), \nabla \otimes \tilde{\mathbf{u}})_{L_2(\Omega)}, \tag{22}$$

hence Eq. (20) becomes

$$c_k(\tilde{\mathbf{u}}) = \frac{F^{(k)}(s)}{m_k(s^2 + \omega_k^2)}. \tag{23}$$

Then the displacement field $\tilde{\mathbf{u}}$ is expressed, using Eqs. (8) and (23), by the modal model

$$\tilde{\mathbf{u}}(\mathbf{x}, s) = \sum_{k=1}^{\infty} \frac{F^{(k)}(s)}{m_k(s^2 + \omega_k^2)} \mathbf{w}^{(k)}(\mathbf{x}). \tag{24}$$

2.5. Truncated response model

In applications, only a finite number of approximations of the modes, $\mathbf{w}^{(k)}$, are available, therefore it is necessary to truncate the infinite series, as in Eqs. (8) and (11). Then a finite-dimensional model for boundary traction vector estimation using measured vibration responses can be derived. This truncation will result in an error of the estimated Fourier coefficients. Note, however, that the estimated displacement vector (based on the estimated Fourier coefficients) converges to the true one in an $L_2(\Omega)$-norm, see e.g., Ref. [17].

Now assume that up to K number of modes are to be used in the traction vector estimation technique, as described below. Then, for the measured response, $\tilde{U}_i^{mea}$, at a point $p(j)$ with co-ordinate $\mathbf{x}_{p(j)}$ and measurement direction $\mathbf{n}_i$ ($\mathbf{n}_i$ being a unit three-dimensional vector), Eq. (24) provides the following relationship:

$$\tilde{\mathbf{U}}^{mea} = \mathbf{A}\mathbf{C} + \tilde{\mathbf{U}}^{res}, \tag{25}$$

where $\mathbf{A}$ is a real and constant $N \times K$ response matrix (N being the number of measured responses), with components defined as

$$A_{ik} \coloneqq \mathbf{n}_i \cdot \mathbf{w}^{(k)}(\mathbf{x}_{p(j)}) \tag{26}$$

relating the Fourier coefficients, arranged in $\mathbf{C}$, to the displacements; $\mathbf{C}$ is defined such that

$$\mathbf{C} \coloneqq [c_1(\tilde{\mathbf{u}}), c_2(\tilde{\mathbf{u}}), \ldots, c_K(\tilde{\mathbf{u}})]^{\mathrm{T}}. \tag{27}$$

Note that at each point $p(j)$ there can be up to three responses, $\tilde{U}_i^{mea}$, i.e., if measurements are made in more than one direction at $p(j)$. Hence, $j \in \{1, \ldots, P\}$, $P \leqslant N$.

Finally $\tilde{\mathbf{U}}^{res}$, in Eq. (25), is the residual caused by truncation of the infinite series as in Eq. (24). It is defined by the components

$$\tilde{U}_i^{res} \coloneqq \sum_{k=K+1}^{\infty} \frac{F^{(k)}}{m_k(s^2 + \omega_k^2)} \mathbf{n}_i \cdot \mathbf{w}^{(k)}(\mathbf{x}_{p(j)}). \tag{28}$$

Since the objective here is to calculate the modal force, caused by some unknown excitation/reaction, only the contribution to the modal force from some known excitation can be calculated; also, when no excitation is known the complete residual is neglected.

Now least square estimates of the Fourier coefficients, $c_k(\tilde{\mathbf{u}})$, can be obtained by means of Eqs. (25)–(28), i.e., $\mathbf{C}$ can be estimated by

$$\mathbf{C}_{est} = \mathbf{A}^{+}(\tilde{\mathbf{U}}^{mea} - \tilde{\mathbf{U}}^{res}), \tag{29}$$

where $\mathbf{A}^{+} \coloneqq (\mathbf{A}^{\mathrm{T}}\mathbf{A})^{-1}\mathbf{A}^{\mathrm{T}}$ is the pseudo-inverse of $\mathbf{A}$. Thereafter, $\{F^{(k)}(s)\}_{k=1}^{K}$ is easily obtained by use of Eq. (23). Note that responses can be predicted at arbitrary points, i.e., even at points not measured, in the structure by use of the set of calculated $\{F^{(k)}(s)\}_{k=1}^{K}$ and Eq. (24).

3. Traction vector estimation methods

Given the set of modal forces, $\{F^{(k)}\}_{k=1}^{K}$, obtained by the least square technique described in the previous section, the traction vector can be estimated. This can be done in several ways. Three estimation methods as proposed by Sehlstedt [1–3] will be outlined in Sections 3.1–3.3, respectively.

Let $\partial\Omega_c$, $\partial\Omega_c \subseteq \partial\Omega$, be the surface where the traction vector is sought. Then the traction vector can be estimated by means of Eq. (19) from the set of estimated modal forces as

$$F^{(k)}(s) = (\tilde{\mathbf{t}}_n, \mathbf{w}^{(k)})_{\mathrm{L}_2(\partial\Omega_c)}, \quad k = 1, \ldots, K. \tag{30}$$

This is theoretically straightforward. In many applications though, the system of equation that arises is often ill-conditioned. This was shown in Ref. [1] to be caused by the fact that modes orthogonal in Ω is not, in general, orthogonal on the surface of interest $\partial\Omega_c$. However, there may exist a subset of the set of available modes which are orthogonal, or nearly orthogonal. This is the basis of the techniques in Refs. [1–3].

The selection of modes can be done in several ways; one way is to use an algorithm that minimizes the condition number. This will be adapted in this paper.

In Section 3.1, Eq. (30) will be solved by using FE-interpolation for the traction vector and eigenmodes. The technique in Section 3.2 will, instead of FE-interpolation for the traction field, use a series expansion of the stress tensor. This is further extended in Section 3.3 to utilize a set of surface orthogonal basis functions as a basis for the traction vector series expansion.

3.1. Method based on FE-interpolation

Here the technique in Ref. [1] will be briefly summarized.

To be able to solve Eq. (30), some appropriate spatial interpolation is needed for the traction vector field, $\tilde{\mathbf{t}}_n$. If the eigenmodes are calculated using the finite element method (FEM) the spatial interpolation for the eigenmodes, $\mathbf{w}^{(k)}$ are already determined. Then, in each FE element, the traction vector and eigenmode can be expressed as

$$\tilde{\mathbf{t}}_n(\mathbf{x}, s) = \mathbf{A}_e(\mathbf{x})\tilde{\mathbf{T}}_e(s), \tag{31}$$

$$\mathbf{w}^{(k)}(\mathbf{x}) = \mathbf{A}_e(\mathbf{x})\mathbf{W}_e^{(k)}, \tag{32}$$

where $\mathbf{A}_e(\mathbf{x})$ is the element spatial FE-interpolation matrix. $\tilde{\mathbf{T}}_e(s)$ and $\mathbf{W}_e^{(k)}$ are the discrete element traction and eigenmode vectors, respectively

Using numerical integration, Eq. (30) can be expressed as

$$F^{(k)}(s) = \mathbf{Q}^{(k)}\tilde{\mathbf{T}}(s), \tag{33}$$

$$\mathbf{Q}^{(k)} = \sum_{e=1}^{N_{\partial\Omega_c}} (\mathbf{W}_e^{(k)})^{\mathrm{T}} \left[\int_{\partial\Omega_{c,e}} \mathbf{A}_e^{\mathrm{T}} \mathbf{A}_e \, \mathrm{d}\partial\Omega \right] \mathbf{\Lambda}_e, \tag{34}$$

where $\tilde{\mathbf{T}}(s)$ is the global column traction vector of the surface, $N_{\partial\Omega_c}$ is the number of elements on the surface $\partial\Omega_c$, and $\mathbf{\Lambda}_e$ is an incidence matrix relating the local degrees of freedom for element e to the global degrees of freedom.

If the estimated modal contact forces, $F^{(k)}(s)$, is arranged in a column vector, $\mathbf{F}(s)$, such that

$$\mathbf{F}(s) = [F^{(1)}(s), F^{(2)}(s), \ldots, F^{(K)}(s)]^{\mathrm{T}} \tag{35}$$

and, using Eqs. (33) and (34), a matrix $\mathbf{Q}$ can be defined such that

$$\mathbf{Q}^{\mathrm{T}} \coloneqq [(\mathbf{Q}^{(1)})^{\mathrm{T}}, (\mathbf{Q}^{(2)})^{\mathrm{T}}, \ldots, (\mathbf{Q}^{(K)})^{\mathrm{T}}], \tag{36}$$

and

$$\mathbf{F}(s) = \mathbf{Q}\tilde{\mathbf{T}}(s), \tag{37}$$

i.e., row K in $\mathbf{Q}$ consists of Eq. (34) with $k = K$.

Now the key issue here is to overcome the problem of ill-conditioning, which is caused by the lack of orthogonality of the eigenmodes, as mentioned in the introduction of Section 3, at the specific subsection of the structure, and therefore causing the matrix $\mathbf{Q}$ to be ill-conditioned. Consider a sub-matrix, $\mathbf{Q}_\beta$, consisting of rows in $\mathbf{Q}$ that are not linearly dependent. This approach may yield a low condition number for $\mathbf{Q}_\beta$. Then with the corresponding sub-vector of $\mathbf{F}$ denoted $\mathbf{F}^\beta$

$$\tilde{\mathbf{T}}(s) = \mathbf{Q}_\beta^{+}\mathbf{F}^\beta, \tag{38}$$

where $\mathbf{Q}_\beta^{+}$ is the pseudo-inverse of $\mathbf{Q}_\beta$.

3.2. Method based on stress tensor expansion

In this section the method in Ref. [2] will be outlined.

By utilizing Eqs. (7), (11)–(13) and (30) the following series representation is obtained:

$$F^{(k)}(s) = \sum_{l=1}^{\infty} g_l(\tilde{\boldsymbol{\sigma}}) R_{kl}, \tag{39}$$

where

$$R_{kl} \coloneqq ((\mathscr{H}_e : \boldsymbol{\varepsilon}_\sigma^{(l)})\mathbf{n}, \mathbf{w}_u^{(k)})_{\mathrm{L}_2(\partial\Omega_c)} = (\mathbf{t}_{n,\sigma}^{(l)}, \mathbf{w}_u^{(k)})_{\mathrm{L}_2(\partial\Omega_c)}, \tag{40}$$

where $\mathbf{t}_{n,\sigma}^{(l)}$ is the elastic traction vector corresponding to the elastic strain mode $\boldsymbol{\varepsilon}_\sigma^{(l)}$.

The system of Eqs. (39) can be expressed in infinite matrix format as

$$\begin{bmatrix} F_c^{(1)} \\ F_c^{(2)} \\ \vdots \\ F_c^{(k)} \\ \vdots \end{bmatrix} = \begin{bmatrix} R_{11} & R_{12} & \cdots & R_{1l} & \cdots \\ R_{21} & R_{22} & \cdots & R_{2l} & \cdots \\ \vdots & \vdots & \ddots & \vdots & \ddots \\ R_{k1} & R_{k2} & \cdots & R_{kl} & \cdots \\ \vdots & \vdots & \ddots & \vdots & \ddots \end{bmatrix} \begin{bmatrix} g_1 \\ g_2 \\ \vdots \\ g_l \\ \vdots \end{bmatrix}, \tag{41}$$

$$\Leftrightarrow$$

$$\mathbf{F}_c = \mathbf{R}\mathbf{G}. \tag{42}$$

The problem of estimating the frequency-dependent traction vector field, $\tilde{\mathbf{t}}_n(\mathbf{x}, s)$, at points $\mathbf{x}$ on the boundary $\partial\Omega_c$ is reduced to estimating the frequency-dependent Fourier coefficients $\{g_l(\tilde{\boldsymbol{\sigma}})\}_{l=1}^{\infty}$ by means of Eq. (42).

The ill-conditioning is overcome by choosing, using e.g., an algorithm that minimizes the condition number, a set of modes which are orthogonal, or almost orthogonal, over the boundary in question a sub-matrix, $\mathbf{R}_\beta$, of the complete system matrix $\mathbf{R}$ can be obtained. The rows in $\mathbf{R}_\beta$ correspond to the set of modes orthogonal over the boundary in question. Then, by means of a sub-vector, $\mathbf{F}_c^\beta$, of the modal force vector, $\mathbf{F}_c$, corresponding to the matrix $\mathbf{R}_\beta$, the following system of equations are given:

$$\mathbf{F}_c^\beta = \mathbf{R}_\beta \mathbf{G}. \tag{43}$$

Now, by taking the pseudo-inverse, $\mathbf{R}_\beta^+$, of $\mathbf{R}_\beta$ the Fourier coefficients of the stress series (contained in the vector $\mathbf{G}$) can be estimated

$$\mathbf{G}_{est} = \mathbf{R}_\beta^+ \mathbf{F}_c^\beta. \tag{44}$$

Then by means of Eqs. (7), (11)–(13) and the set of estimated stress series Fourier coefficients, $\mathbf{G}_{est}$, the boundary traction vector can be calculated at arbitrary points in $\partial\Omega_c$.

The choice of boundary conditions for the eigenvalue problems, when calculating the eigenmodes sets $\{\mathbf{w}_u^{(k)}\}_{k=1}^{\infty}$ and $\{\mathbf{w}_\sigma^{(l)}\}_{l=1}^{\infty}$, requires some further explanations. Regarding the eigenmodes (or basis functions), $\mathbf{w}_u^{(k)}$, for the displacement series, Eq. (8), it is important to note that on parts of the boundary, $\partial\Omega_c \subseteq \partial\Omega$, where the traction vector, $\tilde{\mathbf{t}}_n$, is sought, the required boundary condition for the elastic eigenvalue problem *must* be an homogeneous *elastic* traction field, i.e., $\mathbf{t}_n^{(k)} = (\mathscr{H}_e : \boldsymbol{\varepsilon}_u^{(k)})\mathbf{n} \equiv \mathbf{0}$. Hence the boundary $\partial\Omega_t$ *must* contain $\partial\Omega_c$, i.e., $\partial\Omega_c \subset \partial\Omega_t$, otherwise, *no* information about the sought boundary traction vector, $\tilde{\mathbf{t}}_n$, can be extracted. Recall that $\mathbf{t}_n^{(k)}$ is the elastic traction vector corresponding to the elastic strain tensor mode, $\boldsymbol{\varepsilon}_u^{(k)}$, for a specific direction defined by the unit normal $\mathbf{n}$, and $\boldsymbol{\varepsilon}_u^{(k)}$ in turn corresponds to the elastic displacement mode, $\mathbf{w}_u^{(k)}$, by Eq. (A.15).

For the basis functions $\boldsymbol{\sigma}^{(l)}$ in the stress series, as in Eq. (11) and defined according to Eqs. (12)–(13), the eigenvalue problem must be defined such that $\sigma_{ij}^{(l)}(\mathbf{x}) \neq 0$ for certain $ij \in \{11, 22, 33, 12, 23, 31\}$, $l \in \mathbb{N}$ and $\mathbf{x} \in \partial\Omega_c$, i.e., the stress basis functions must be such that they can represent non-homogeneous stress tensor components, $\tilde{\sigma}_{ij} \neq 0$, on $\partial\Omega_c$. Hence the boundary conditions for the eigenvalue problem *must* be an homogeneous displacement mode field, i.e. $\mathbf{w}^{(l)} \equiv \mathbf{0}$, on $\partial\Omega_c$. Thus $\partial\Omega_c \subseteq \partial\Omega_w$.

3.3. Method based on construction of an orthogonal basis

Here the technique in Ref. [3] will be summarized.

Let $\{\mathbf{v}^{(l)}(\mathbf{x})\}_{l=1}^{\infty}$ be a normalized, orthogonal sequence of basis function over the surface $\partial\Omega_c \subseteq \partial\Omega$, constructed as in Section 2.3. Then the frequency domain traction vector on the surface $\partial\Omega_c$ can be expressed as

$$\tilde{\mathbf{t}}_n(\mathbf{x}, s) = \sum_{l=1}^{\infty} h_l(\tilde{\mathbf{t}}_n)\mathbf{v}^{(l)}(\mathbf{x}) \quad \text{for } \mathbf{x} \in \partial\Omega_c, \tag{45}$$

where $\{h_l(\tilde{\mathbf{t}}_n)\}_{l=1}^{\infty}$ are Fourier coefficients defined as

$$h_l(\tilde{\mathbf{t}}_n) \coloneqq (\tilde{\mathbf{t}}_n, \mathbf{v}^{(l)})_{\mathrm{L}_2(\partial\Omega_c)}. \tag{46}$$

By means of Eqs. (19) and (45) the following can be obtained:

$$F^{(k)}(s) = \sum_{l=1}^{\infty} S_{kl} h_l, \tag{47}$$

where

$$S_{kl} \coloneqq (\mathbf{v}^{(l)}, \mathbf{w}^{(k)})_{\mathrm{L}_2(\partial\Omega_c)}. \tag{48}$$

The above give rise to an infinite system of equations as below

$$\begin{bmatrix} F^{(1)} \\ F^{(2)} \\ \vdots \\ F^{(k)} \\ \vdots \end{bmatrix} = \begin{bmatrix} S_{11} & S_{12} & \cdots & S_{1l} & \cdots \\ S_{21} & S_{22} & \cdots & S_{2l} & \cdots \\ \vdots & \vdots & \ddots & \vdots & \ddots \\ S_{k1} & S_{k2} & \cdots & S_{kl} & \cdots \\ \vdots & \vdots & \ddots & \vdots & \ddots \end{bmatrix} \begin{bmatrix} h_1 \\ h_2 \\ \vdots \\ h_l \\ \vdots \end{bmatrix}, \tag{49}$$

$$\Leftrightarrow$$

$$\mathbf{F} = \mathbf{S}\mathbf{H}. \tag{50}$$

Given the set of coefficients for the traction series, $\{h_l(\tilde{\mathbf{t}}_n)\}_{l=1}^{\infty}$, the traction vector, $\tilde{\mathbf{t}}_n = \tilde{\mathbf{t}}_n(\mathbf{x}, s)$, at the surface of interest, $\partial\Omega_c$, can easily be obtained from Eq. (45).

Now, as before, by choosing, using e.g., an algorithm that minimizes the condition number, a set of modes which are orthogonal, or almost orthogonal, over the boundary in question a sub-matrix, $\mathbf{S}_\beta$, of the complete system matrix $\mathbf{S}$ can be obtained. The rows in $\mathbf{S}_\beta$ correspond to the set of modes orthogonal over the boundary in question. Then, by means of a sub-vector, $\mathbf{F}_\beta$, of the modal force vector, $\mathbf{F}$, corresponding to the matrix $\mathbf{S}_\beta$, the following system of equations are given:

$$\mathbf{F}_\beta = \mathbf{S}_\beta \mathbf{H}. \tag{51}$$

Now, by taking the pseudo-inverse, $\mathbf{S}_\beta^+$, of $\mathbf{S}_\beta$ the Fourier coefficients of the traction vector series (contained in the vector $\mathbf{H}$) can be estimated

$$\mathbf{H}_{est} = \mathbf{S}_\beta^+ \mathbf{F}_\beta. \tag{52}$$

Then by means of Eq. (45) and the set of estimated traction series Fourier coefficients, $\mathbf{H}_{est}$, the boundary traction vector can be calculated at arbitrary points in $\partial\Omega_c$.

Separate traction series with separate basis functions are needed if the surface of interest, $\partial\Omega_c$, is composed by disjoint partial surfaces. For example if L basis functions are used in each truncated traction series, then the length of the vector $\mathbf{H}$ is L times the number of partial surfaces.

3.4. Discussion of differences between the techniques

As can be seen in this section, the methods are all based on estimation of the Fourier coefficients for the displacement series, or more precisely the corresponding modal forces. But that is where the similarities end.

The technique described in Section 3.1 utilizes FE-interpolation of both the traction vector and eigenmode vector. This will, usually, result in an under-determined system of equations, due to the fact that the number of traction FE-components are, usually, higher than the set of eigenmodes.

For the methods in Sections 3.2 and 3.3 this is not the case. Here there are overdetermined systems of equations, due to the number of basis functions for in the stress series respectively the traction series expansion can be chosen smaller than the number of basis functions for the displacement series. One big advantage of the technique in Section 3.3 over the one in Section 3.2 is that the basis functions are *truly* orthogonal over the surface of interest.

4. Experimental test case

In this section experimental validation of the techniques described in the previous section will be made.

The test structure consists of an aluminum plate structure squeezed between two steel supports, which in turn are clamped to a rigid body, see Fig. 1 where the support on one side is depicted. The other support is located on the opposite side (with respect to the z-axis) of the plate. The dimensions of the aluminum plate are $0.3 \times 0.52 \times 0.0042$ m ($x \times y \times z$); the dimensions of the

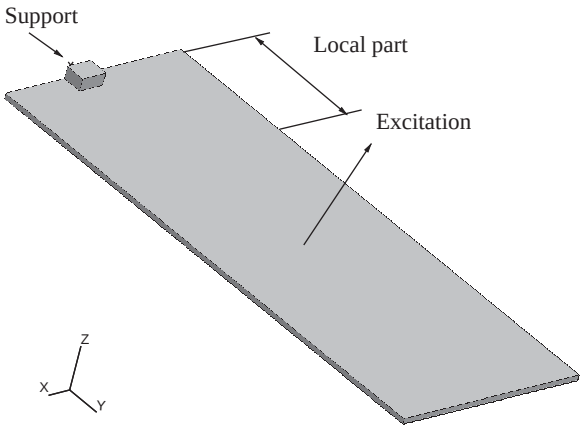

Fig. 1. The experimental test setup.

steel supports are $0.04 \times 0.02 \times 0.02$ m ($x \times y \times z$). The contact surfaces between the supports and the plate are

$$\partial\Omega_{c,1} \coloneqq \{\mathbf{x} | x \in [0.16, 0.2], y \in [0.0, 0.02], z = 0.0\} \cup \{\mathbf{x} | x \in [0.16, 0.2], y \in [0.0, 0.02], z = 0.0042\}. \tag{53}$$

The structure is excited by a traction vector field $\tilde{\mathbf{t}}_n(\mathbf{x}_e, s) = [0, 0, 1]^{\mathrm{T}}$ Pa, approximating a concentrated load at $\mathbf{x}_e = [0.14, 0.26, 0.0]$ m.

The elastic material properties for the aluminum plate are $\rho_{Al} = 2795\ \mathrm{kg/m^3}$ for the mass distribution, and zero frequency Young's modulus and Poisson's ratio $E_{Al} = 73.0$ GPa and $\nu_{Al} = 0.3260$, respectively.

The analysis will be performed on a sub-structure of the plate, called the *local part* (see Fig. 1). The local part is the first (measured from $y = 0.0$) 0.2 m in the y-direction of the aluminum beam. Thus, with the notation in this paper

$$\Omega \coloneqq \{\mathbf{x} | x \in [0.0, 0.3],\ y \in [0.0, 0.2],\ z \in [0.0, 0.0042]\}. \tag{54}$$

The internal surface between the local part and the rest of the plate is defined as

$$\partial\Omega_{c,2} \coloneqq \{\mathbf{x} | x \in [0.0, 0.3],\ y = 0.2,\ z \in [0.0, 0.0042]\}. \tag{55}$$

The traction vector is then sought at the contact surfaces between the plate and the support and the internal surface between the local part and the rest of the plate. With the notation in this paper: $\partial\Omega_c = \partial\Omega_{c,1} \cup \partial\Omega_{c,2}$.

Measurements are carried out on the local part only and only on one side of the plate ($z = 0.0042$). The measurements are obtained by means of a laser Doppler vibrometer (LDV) and a triaxial accelerometer. The total number of measurement points are 280 (140 LDV points and 140 accelerometer points) evenly distributed over the local part so that they can resolve the shortest wavelength in the eigenmode base for the displacement series. The tri-axial measurements are vital for the techniques to work. Thus, the accelerometer could be used for all measurement points; however, based on the fact that the structure is a plate the number of lateral measurements can be reduced and therefore only information on displacements normal to the plate is sufficient at some points. This is the reason that LDV is used to complement the accelerometer measurements. The brand of the accelerometer is Endevco and the type is Model 23. The accelerometer is very small and has a very low weight of 0.8 g and it is assumed that its influence to the vibration field of the structure neglectable.

Ultimately, all of the measurements should be performed using non-contact techniques. Some research results within the field of measurement techniques, such as Ref. [18], pose promising developments toward this goal. However, it must be emphasized that such techniques are not yet industrially applicable.

It is necessary to solve the eigenvalue problem to obtain the basis for the displacement series (as in Eq. (8)). Since there are no parts with essential boundary conditions on the local part, $\partial\Omega_w = \emptyset$ (in Eq. (A.14)) and $\partial\Omega_t = \partial\Omega$ (in Eq. (A.13)), corresponding to a homogeneous pure Neumann problem; in other words a free structure. The eigenvalue problem is solved by means of MSC Nastran$^{\mathrm{TM}}$ for 430 eigenmodes. Eigenmode number 430 is depicted in Fig. 2. The finite element mesh consists of 60 000 hexahedral elements with 8 node points in each equalling a total of 76 255 node points in the local part. The elements are all of the same size and distributed accordingly: 150

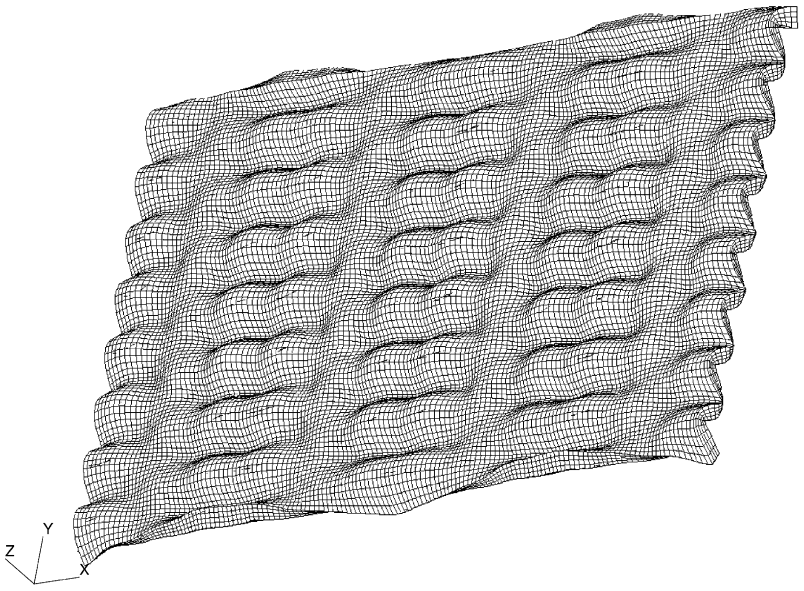

Fig. 2. Mode number 430.

elements along the x-axis, 100 elements along the y-axis and 4 elements along the z-axis. This will yield 462 node points at the surface $\partial\Omega_{c,1}$ and 755 node points at the surface $\partial\Omega_{c,2}$, equalling a total of 1217 node points on $\partial\Omega_c$.

The choice of total number of eigenmodes (430), is governed by the geometrical extent of the contact area. The minimum requirement is that at least half of one eigenmode wave should cover the contact area. Here the wavelength for eigenmode 430 is approximately 3.8 cm and the shortest length of the contact area is 2 cm.

Now it is straightforward to calculate the components of the matrix $\mathbf{A}$, defined in Eq. (26). Thereafter, mean square estimates of the Fourier coefficients for the displacement series is obtained using Eq. (29).

The estimated set of Fourier coefficients $\{c_k(\tilde{\mathbf{u}})\}_{k=1}^{430}$ is validated using independently measured displacement, i.e. displacement not used in the coefficient estimation, which can be seen in Figs. 3 and 4 for the y- and z-components at $\mathbf{x} = [0.06, 0.04, 0.00]$ m, respectively.

Then it is straightforward to calculate the set of modal contact forces $\{F_c^{(k)}\}_{k=1}^{430}$ from the set of estimated Fourier coefficients, $\{c_k(\tilde{\mathbf{u}})\}_{k=1}^{430}$, using Eq. (23).

Now using FE-interpolation for both the traction field at $\partial\Omega_c$ and the eigenmodes the traction vector can be estimated using the technique described in Section 3.1.

To obtain results using the method in Section 3.2 an auxiliary eigenvalue problem needs to be solved, in order to obtain the basis for the stress series (Eq. (11)). The boundary domains are chosen such that $\partial\Omega_w = \partial\Omega_c$ and $\partial\Omega_t = \partial\Omega \backslash \partial\Omega_c$. This will yield a basis, $\{\boldsymbol{\sigma}^{(l)}\}_{l=1}^{\infty}$, that can represent $\tilde{\sigma}_{ij}(\mathbf{x}, s) \neq 0$ at $\mathbf{x} \in \partial\Omega_c$. As previously the eigenvalue problem is solved by means of MSC Nastran^{TM}. Now the components of the matrix $\mathbf{R}$ can be calculated using Eq. (40). Thereafter, following the discussion in Section 3.2, we choose a subset of the set of available displacement modes ($k \in \{1, \ldots, 430\}$) so that the matrix $\mathbf{R}_\beta$ becomes well-conditioned enough.

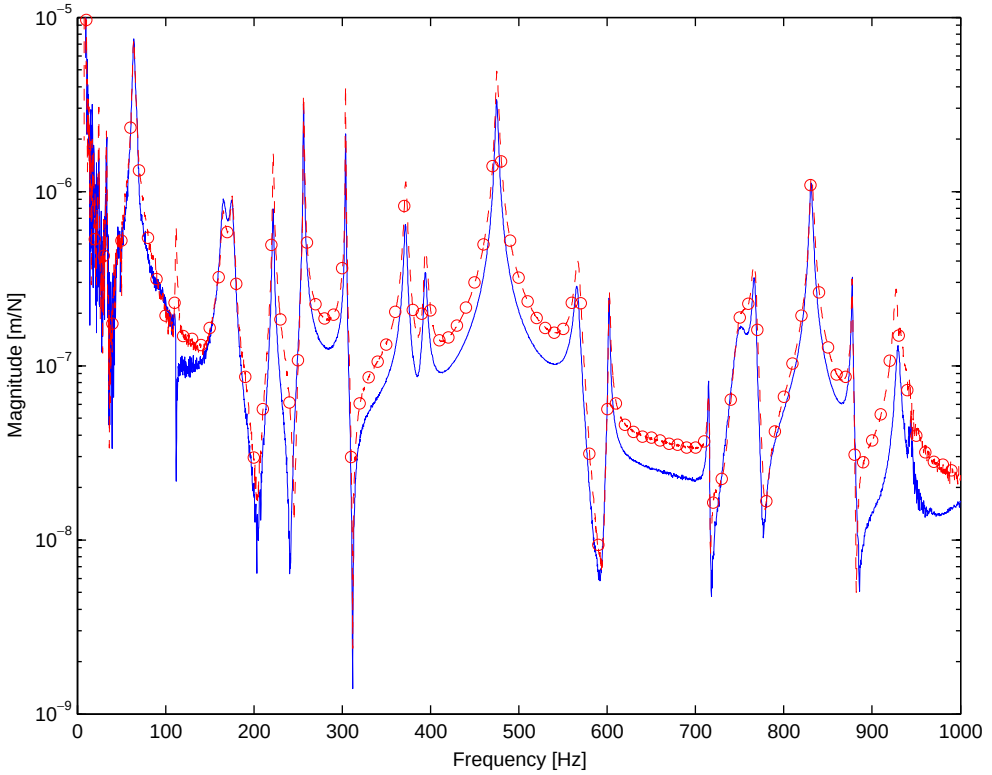

Fig. 3. Validation of independently measured displacement spectrum in the y-direction at $\mathbf{x} = [0.06, 0.04, 0.00]$: —, measured; -○-, estimated.

To proceed with the third method, as described in Section 3.3, we need to obtain an set of basis functions orthogonal over $\partial\Omega_c$. This is done using the orthogonalization procedure outlined in Section 2.3 and the eigenmodes obtained from the first eigenvalue problem above. Now the traction vector can be estimated using the technique in Section 3.3.

The, by means of the three above-mentioned methods, estimated traction vectors are compared in a number of points in the structure. This comparison can be seen in Figs. 5–8. By keeping in mind that the number of traction vector components is $1217 \times 3 = 3651$, the results are fairly good. Also comparison in a $L_2(\partial\Omega_c)$-norm over the surface is made between the three techniques and depicted in Fig. 9. As can be seen the results are very good.

5. Conclusions

Three previously proposed techniques are experimentally validated using LDV measurements combined with triaxial accelerometer measurements on a constrained vibrating structure. The techniques utilize the measurements and certain elastic eigenmodes in order to yield the detailed (in a spatial sense) traction vector at relevant surfaces. Comparison between the three methods has been made both pointwise and in a L_2-norm over the surface. There are some discrepancies

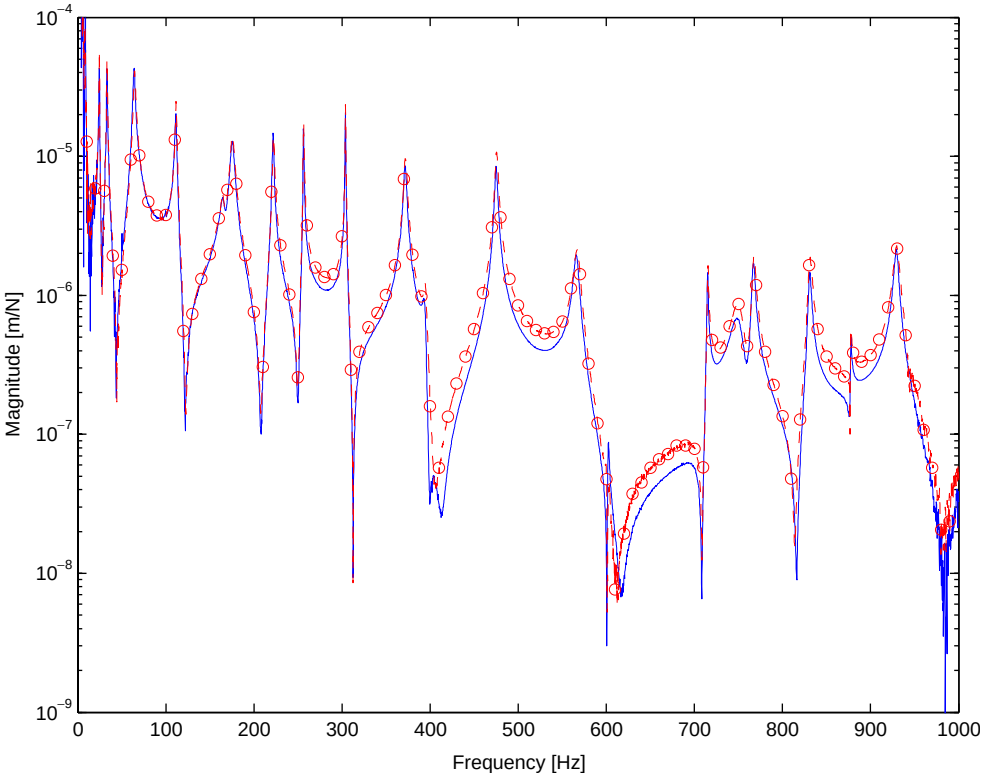

Fig. 4. Validation of independently measured displacement spectrum in the z-direction at $\mathbf{x} = [0.06, 0.04, 0.00]$: —, measured; -○-, estimated.

regarding the pointwise comparison. However when regarding the large number of estimated traction components these discrepancies are fairly small. In the L_2-norm the methods correspond very well.

These results yield that the methods are very promising as starting points for research focusing on deriving physical models describing the dissipation of vibration energy between structural parts. This area is usually referred to as non-material damping and is an area that requires extensive research since there are very few results available, especially regarding general models.

Acknowledgements

This work was performed under Contract SAP1 FoT-25 2002 from the Swedish Defence Material Administration (FMV). The funding provided is gratefully acknowledged. The authors would like to thank Adam Zdunek and Ulf Tengzelius at the Structural Dynamics research group, Department of Structures and Materials, Aeronautics Division, Swedish Defence Research Agency, for advice, support and encouragement.

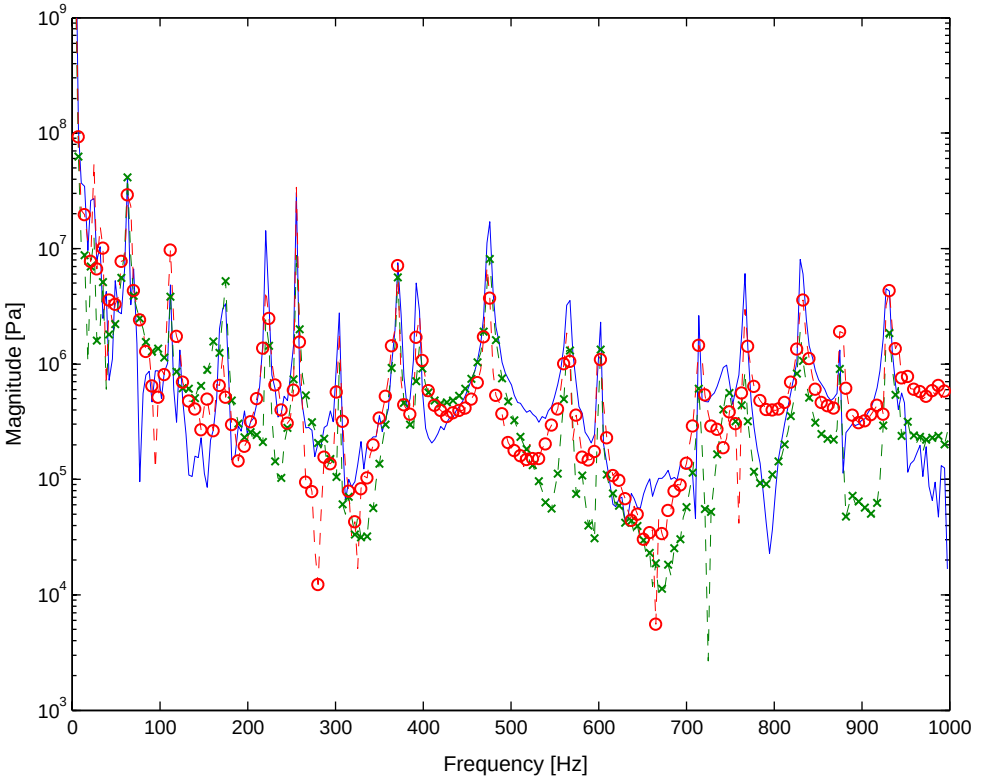

Fig. 5. Comparison between traction estimation methods; magnitude of the x-component at $\mathbf{x} = [0.162, 0.20, 0.00]$ m: —, FE-interpolation method; -×-, stress tensor expansion method; -○-, surface orthogonal basis method.

Appendix A. Definitions

The displacement field, $\mathbf{u}$, the symmetric stress, $\boldsymbol{\sigma}$, and strain tensor fields, $\boldsymbol{\varepsilon}$, in Cartesian co-ordinates are defined as

$$\mathbf{u} \coloneqq \mathbf{u}(\mathbf{x}, t) = [u_x \; u_y \; u_z]^{\mathrm{T}}, \tag{A.1}$$

$$\boldsymbol{\sigma} \coloneqq \boldsymbol{\sigma}(\mathbf{x}, t) = \begin{bmatrix} \sigma_{xx} & \sigma_{xy} & \sigma_{zx} \\ \sigma_{xy} & \sigma_{yy} & \sigma_{yz} \\ \sigma_{zx} & \sigma_{yz} & \sigma_{zz} \end{bmatrix}, \tag{A.2}$$

$$\boldsymbol{\varepsilon} \coloneqq \boldsymbol{\varepsilon}(\mathbf{x}, t) = \begin{bmatrix} \varepsilon_{xx} & \varepsilon_{xy} & \varepsilon_{zx} \\ \varepsilon_{xy} & \varepsilon_{yy} & \varepsilon_{yz} \\ \varepsilon_{zx} & \varepsilon_{yz} & \varepsilon_{zz} \end{bmatrix}, \tag{A.3}$$

where $\mathbf{x} = [x, y, z]^{\mathrm{T}}$ and t is the time variable.

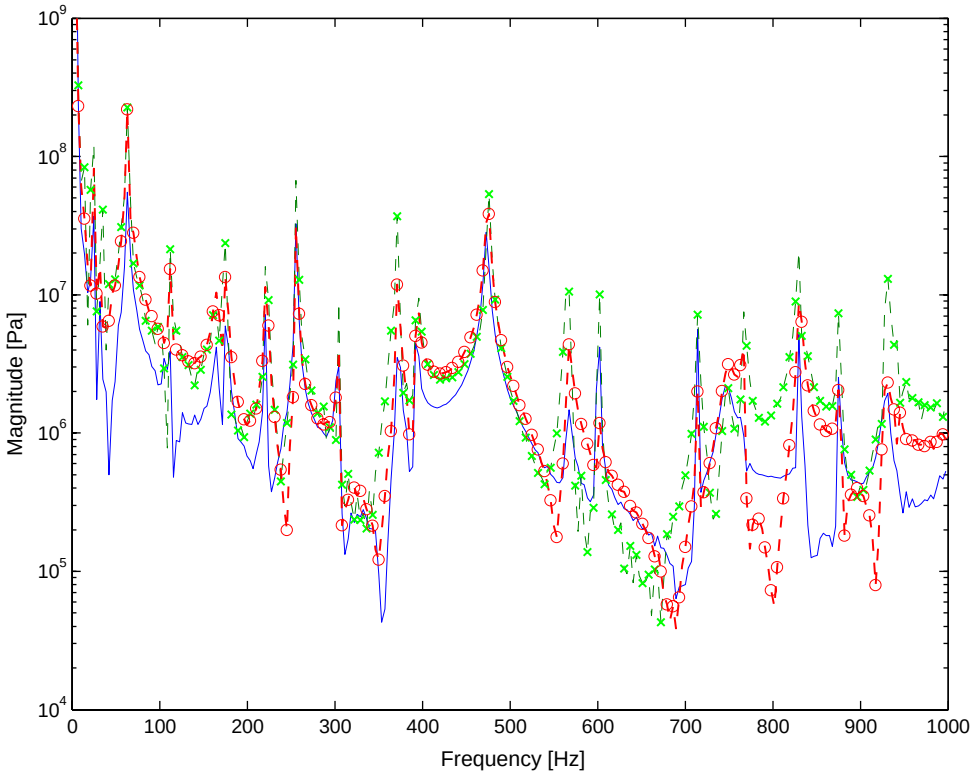

Fig. 6. Comparison between traction estimation methods; magnitude of the z-component at $\mathbf{x} = [0.22, 0.20, 0.0042]$ m: —, FE-interpolation method; -×-, stress tensor expansion method; -○-, surface orthogonal basis method.

The linear strain–displacement field relations are given in tensor notation as

$$\boldsymbol{\varepsilon} = \tfrac{1}{2}[(\nabla \otimes \mathbf{u})^{\mathrm{T}} + \nabla \otimes \mathbf{u}], \tag{A.4}$$

where $\otimes$ is the tensor product, or dyad.

The $L_2(\Omega)$-inner product $(\mathbf{u}, \mathbf{v})_{L_2(\Omega)}$ is defined as, see e.g., Ref. [17] or Ref. [19]

$$(\mathbf{u}, \mathbf{v})_{L_2(\Omega)} \coloneqq \int_{\Omega} \mathbf{u} \cdot \mathbf{v}^* \, \mathrm{d}\Omega, \tag{A.5}$$

where $\mathbf{u}$ and $\mathbf{v}$ are some (possibly) multi-dimensional continuous vector functions, and $\mathbf{v}^*$ denotes the complex conjugate of the field $\mathbf{v}$. For tensor fields, of the same order, the analogous inner product can be defined as

$$(\mathbf{A}, \mathbf{B})_{L_2(\Omega)} \coloneqq \int_{\Omega} \mathbf{A} : \mathbf{B}^* \, \mathrm{d}\Omega, \tag{A.6}$$

where $\mathbf{A}$ and $\mathbf{B}$ are tensors of the same order.

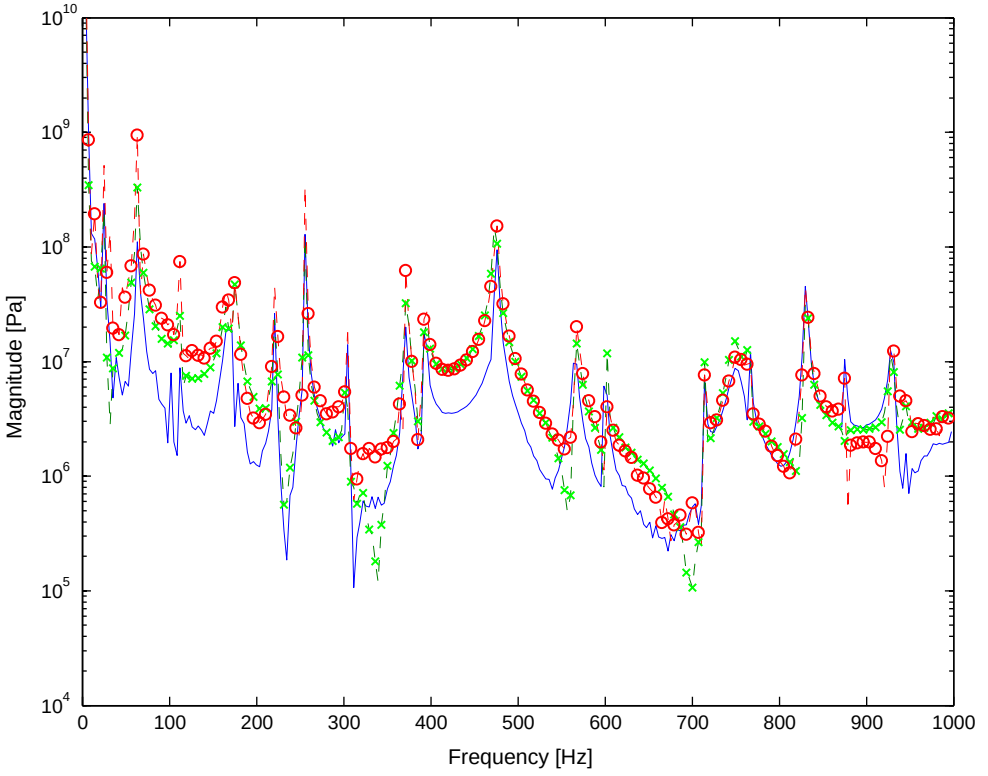

Fig. 7. Comparison between traction estimation methods; magnitude of the z-component at $\mathbf{x} = [0.166, 0.02, 0.0042]$ m: —, FE-interpolation method; -×-, stress tensor expansion method; -○-, surface orthogonal basis method.

The $L_2(\partial\Omega)$-inner product for vector fields on the boundary, $\partial\Omega$, is defined as

$$(\mathbf{u}, \mathbf{v})_{L_2(\partial\Omega)} \coloneqq \int_{\partial\Omega} \mathbf{u} \cdot \mathbf{v}^* \, \mathrm{d}\partial\Omega \tag{A.7}$$

The natural norm in $L_2(\Omega)$ is then defined as

$$\|\mathbf{u}\|_{L_2(\Omega)} \coloneqq \sqrt{(\mathbf{u}, \mathbf{u})_{L_2(\Omega)}} = \sqrt{\int_{\Omega} |\mathbf{u}|^2 \, \mathrm{d}\Omega}. \tag{A.8}$$

The l_2-norm for a n-dimensional, real or complex, vector $\mathbf{y} = [y_1, y_2, \ldots, y_n]$ is defined as

$$\|\mathbf{y}\|_{l_2} \coloneqq \sqrt{\sum_{i=1}^{n} |y_i|^2}. \tag{A.9}$$

When $\mathbf{y}$ is a real vector the above norm is the well-known Euclidean norm. The corresponding l_2-matrix norm for a matrix $\mathbf{A}$, of order $m \times n$, is defined as

$$\|\mathbf{A}\|_{l_2} \coloneqq \sup_{\mathbf{y} \neq \mathbf{0}} \frac{\|\mathbf{A}\mathbf{y}\|_{l_2}}{\|\mathbf{y}\|_{l_2}}. \tag{A.10}$$

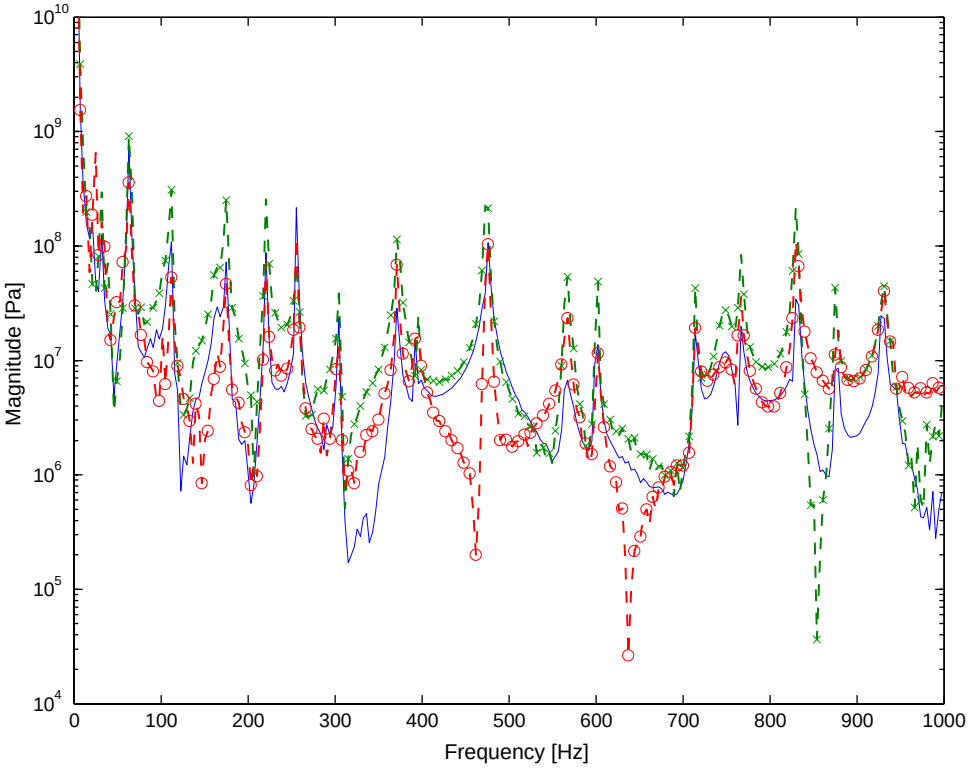

Fig. 8. Comparison between traction estimation methods; magnitude of the y-component at $\mathbf{x} = [0.194, 0.02, 0.0042]$ m: —, FE-interpolation method; -×-, stress tensor expansion method; -○-, surface orthogonal basis method.

The condition number of the matrix $\mathbf{A}$ is defined as

$$\kappa(\mathbf{A}) \coloneqq \|\mathbf{A}\|_{l_2} \, \|\mathbf{A}^+\|_{l_2}, \tag{A.11}$$

where $\mathbf{A}^+$ is the pseudo-inverse of $\mathbf{A}$.

The three-dimensional real valued vector field $\mathbf{w}^{(k)} = [w_x^{(k)}, w_y^{(k)}, w_z^{(k)}]^{\mathrm{T}} \in \mathbb{R}^3$ is the mode shape number k with corresponding circular eigenfrequency ω_k, i.e., $\mathbf{w}^{(k)}$ is assumed to be the solution to an elastic eigenvalue problem with equations of motion

$$-\mathrm{div}(\mathscr{H}_e : \boldsymbol{\varepsilon}^{(k)}) = \omega_k^2 \rho \mathbf{w}^{(k)} \tag{A.12}$$

and homogeneous boundary conditions fulfilling

$$\mathbf{t}_n^{(k)} = \mathbf{0} \quad \text{on } \partial\Omega_t \tag{A.13}$$

$$\mathbf{w}^{(r)} = \mathbf{0} \quad \text{on } \partial\Omega_w \tag{A.14}$$

for all k and r, where $\partial\Omega \coloneqq \partial\Omega_t \cup \partial\Omega_w$. $\boldsymbol{\varepsilon}^{(k)}$ in Eq. (A.12) is the second order strain tensor mode number k corresponding to the displacement mode $\mathbf{w}^{(k)}$ and defined as

$$\boldsymbol{\varepsilon}^{(k)}(\mathbf{w}^{(k)}) \coloneqq \tfrac{1}{2}[(\nabla \otimes \mathbf{w}^{(k)})^{\mathrm{T}} + \nabla \otimes \mathbf{w}^{(k)}]. \tag{A.15}$$

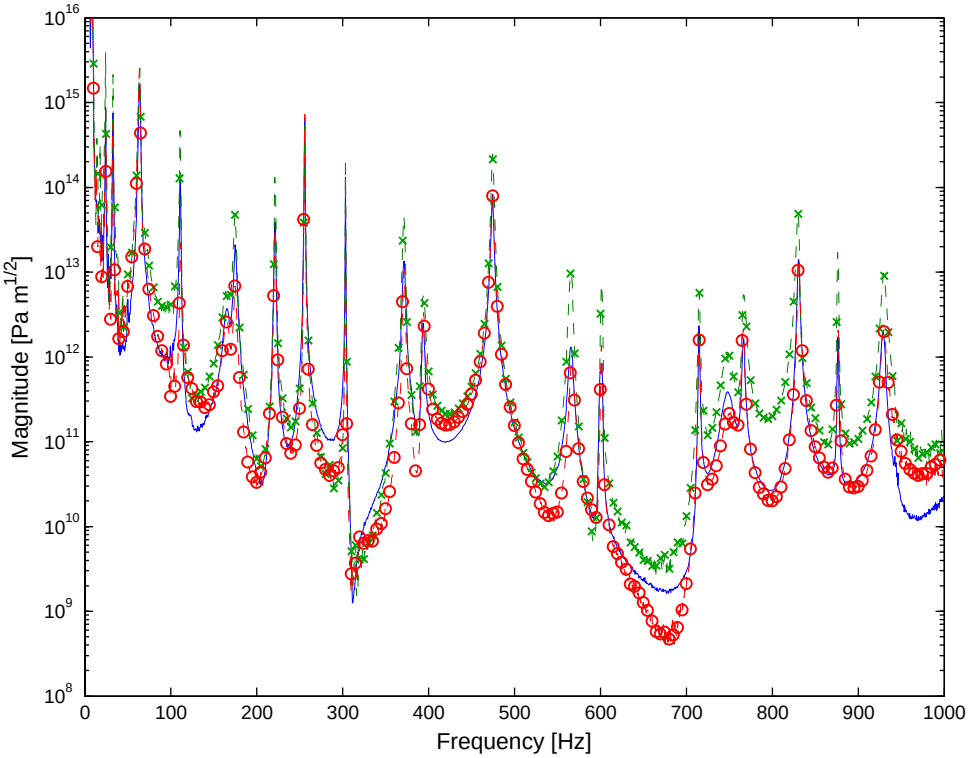

Fig. 9. Boundary norm of the estimated traction vectors for the three different methods: —, FE-interpolation method; -×-, stress tensor expansion method; -○-, surface orthogonal basis method.

It is guaranteed that the continuous (real) modes of vibration constitute a set of complete functions in the Hilbert space $L_2(\Omega)$, cf., Ref. [20], where it was proved for a material continuous body. Here it is assumed to be valid for a material discontinuous body also. In addition to completeness, the modes are orthogonal

$$(\mathbf{w}^{(k)}, \rho\mathbf{w}^{(r)})_{L_2(\Omega)} = m_k \delta_{kr} \quad \forall k, r, \tag{A.16}$$

where δ_{kr} is the Kronecker delta, and $(\,\cdot,\cdot\,)_{L_2(\Omega)}$ is the $L_2(\Omega)$-inner product for a multi-dimensional vector field, as defined in this appendix.

References

[1] N. Sehlstedt, A well-conditioned technique for solving the inverse problem of boundary traction estimation for a constrained vibrating structure, *Computational Mechanics* 30 (2003) 247–258.

[2] N. Sehlstedt, Boundary traction vector estimation in a vibrating structure using series expansion of the stress tensor, *Computational Mechanics*, submitted for publication.

[3] N. Sehlstedt, Construction of three-dimensional orthogonal surface basis functions and well-conditioned boundary traction vector estimation, *Computer Methods in Applied Mechanics and Engineering* 193 (2004) 631–651.

[4] B.J. Dobson, E. Rider, A review of the indirect calculation of excitation forces from measured structural response data, *Proceedings of the Institution of Mechanical Engineers* 204 (1990) 69–75.
[5] P.A. Nelson, S.H. Yoon, Estimation of acoustic source strength by inverse methods: part I, conditioning of the inverse problem, *Journal of Sound and Vibration* 233 (2000) 643–668.
[6] S. Granger, L. Perotin, An inverse method for the identification of a distributed random excitation acting on a vibrating structure, part I: theory, *Mechanical Systems and Signal Processing* 13 (1999) 53–65.
[7] H. Lee, Y. Park, Error analysis of indirect force determination and a regularisation method to reduce force determination error, *Mechanical Systems and Signal Processing* 9 (1995) 615–633.
[8] F.D. Bartlett Jr., W.G. Flannelly, Model verification of force determination for measuring vibratory loads, *Journal of the American Helicopter Society* 24 (1979) 10–18.
[9] J.M. Starkey, G.L. Merrill, On the ill-conditioned nature of indirect force-measurement techniques, *International Journal of Analytical and Experimental Modal Analysis* 4 (1989) 103–108.
[10] M. Hansen, J.M. Starkey, On predicting and improving the condition of modal-model-based indirect force measurement algorithms, *Proceedings of the Eighth IMAC*, Kissimmee, FL, 1990, pp. 115–120.
[11] J. D'Cruz, J.D.C. Crisp, T.G. Ryall, On the force identification of harmonic force on a viscoelastic plate from response data, *Journal of Applied Mechanics* 59 (1992) 722–729.
[12] P.W. Möller, Load identification through structural modification, *Journal of Applied Mechanics* 66 (1999) 236–241.
[13] G.E. Mase, *Continuum Mechanics*, McGraw-Hill, New York, 1970.
[14] G.A. Holzapfel, *Nonlinear Solid Mechanics*, Wiley, Chichester, 2000.
[15] M. Dalenbring, Methods for Experimental Estimation of Anelastic Material Properties, Ph.D. Thesis, Department of Vehicle Engineering, Royal Institute of Technology, Stockholm, Sweden, 2001.
[16] K. Dovstam, Simulation of damped vibrations based on augmented Hooke's law and elastic modes of vibration, *International Journal of Solids and Structures* 37 (2000) 5413–5445.
[17] R.D. Richtmyer, *Principles of Advanced Mathematical Physics*, Vol. I, Springer, New York, 1978.
[18] S. Schedin, G, Pedrini, H.J. Tiziani, F.M. Santoyo, Simultaneous three-dimensional dynamic deformation measurements with pulsed digital holography, *Applied Optics* 38 (1999) 7056–7062.
[19] B.D. Reddy, *Introductory Functional Analysis*, Springer, New York, 1997.
[20] M.E. Gurtin, The linear theory of elasticity, in: S. Flügge, C. Truesdell (Eds.), *Encyclopedia of Physics*, Vol. VIa/2, Mechanics of Solids II, Springer, Berlin, 1972, pp. 1–294.